THE AMERICAN MINERALOGIST, VOL. 53, JULY-AUGUST, 1968

DETERMINATION AND REFINEMENT OF THE STRUCTURE OF HEULANDITE

A. B. MERKLE AND M. SLAUGHTER, *Department of Geology, University of Missouri, Columbia, Missouri.*

ABSTRACT

Heulandite is monoclinic, *Cm*, with unit cell $a=17.73$, $b=17.82$, $c=7.43$Å, $\beta=116°20'$; $Z=4\times$ [(Ca, Na_2) $Al_2Si_7O_{18}\cdot 6H_2O$]. Refinement of the structure of heulandite by the least-squares yields $R=0.14$ and weighted R of 0.11.

Heulandite has well-defined layers formed by 6-, 5-, and 4-member tetrahedral rings lying in *ac*- at 0.25 and 0.75 along *b*-. Open channels are formed by 10-, and 8- member rings which also lie in *ac*- at 0.00 and 0.50 along *b*-. The (010) cleavage is caused by an alternation of the tetrahedral layers and open channels. The structure of heulandite is consistent with Taylor's original concept and with its physical properties.

Al substitutes for Si in 5 of the 9 independent tetrahedra. Average bond distance for Si-O is 1.62 Å, which in aluminum-substituted tetrahedra increases to 1.66 Å.

Heulandite has relatively open channels in three directions. Parallel to *c*-, channels of 10- and 8-member tetrahedral rings have dimensions of 7.05×4.25 Å and 4.60×3.95 Å, respectively. Parallel to *a*-, channels of 8-member rings have dimensions of 5.40×3.90 Å. A third channel formed by 8-member rings is present at an angle of about 50° to the *a*-axis; its dimensions are 5.20×3.90 Å. Two of the three calcium atoms in heulandite occupy positions near the intersection of the 10- and 8-member ring channels, and the third calcium occupies a position at the intersection of two 8-member ring channels. Each calcium atom is coordinated to three framework oxygen atoms and five water molecules. Two of the five water molecules are more closely held by the calcium than the others.

INTRODUCTION

The calcium zeolite heulandite is a widely occurring mineral which is potentially important as a geologic indicator. Heulandite is found in an environment which is saturated or oversaturated with respect to SiO_2 (Coombs, Ellis, Fyfe, and Taylor, 1959). It occurs as an alteration product of acid-igneous rocks or volcanic glass, a cavity filling in basalitc rocks, and as an authigenic mineral in sedimentary rocks. The synthesis of heulandite by Koizumi and Roy (1960) in a limited temperature and pressure range (200°C–360°C at 15,000–37,000 psi) and the destruction of both the natural and artificial mineral at temperatures of 400°C and above, indicates heulandite could be used as a geologic thermometer. The formation of heulandite in a SiO_2-rich environment could also indicate a specific environment of formation which would be useful in studying genesis or alteration of heulandite-bearing rocks.

The determination and refinement of the structure of heulandite was initiated to provide additional information to aid in clarifying its genesis and geologic usefulness. It was also hoped that the knowledge of the crystal structure of heulandite would lead to a better understanding of its ion-exchange properties.

Previous work. The presence of perfect (010) cleavage in heulandite led Taylor (1934) to propose that heulandite is most likely formed by a layered arrangement of silicate tetrahedra. In 1955 Ventriglia made an attempt to solve the crystal structure. Ventriglia's structure differed considerably from Taylor's original concept; it comprised silicate tetrahedra forming a network of 8- and 5-member ring channels in the *ab*-crystallographic plane and network of 6-member ring channels in the *ac*-crystallographic plane. A structural model built from diagrams presented in Ventriglia's paper indicated his structure would not permit an (010) cleavage, did not contain enough independent silicate tetrahedra to be consistent with the chemical contents of the unit cell, and single crystal x-ray diffraction data showed his space group determination was incorrect. Furthermore, interatomic vectors based on his proposed structure were not observed on three-dimensional Patterson maps.

Experimental

Morphology, optical properties and density. The heulandite specimen used in this investigation was from Giebelsbach, near Fiesch, Wallis, Switzerland. Heulandite crystals cover an aggregate of fluorite crystals. Euhedral crystals of heulandite had prominent (010), (101), ($\bar{1}0\bar{1}$), ($\bar{1}0\bar{1}$), and ($10\bar{1}$) forms. Heulandite has perfect (010) cleavage caused by a layering of the silicate tetrahedra comprising its structural framework.

The optical properties of the heulandite specimen, as determined by the immersion method on crushed fragments, are as follows: $\alpha = 1.496$, $\beta = 1.498$, $\gamma = 1.504 \pm 0.001$, biaxial (+), birefringence–0.008, $2V = 35°$, optic axis plane (010). Optical properties determined are consistent with the values $\alpha = 1.491$–1.505, $\beta = 1.493$–1.503, $\gamma = 1.500 - 1.512$ presented in Deer, Howie, and Zussman (1963, p. 376).

The density of heulandite, measured with a Berman balance, was 2.198, the mean of three independent measurements of crystal fragments having an average weight of 15 milligrams. This density compares favorably with the values 2.10–2.20 presented in Deer, Howie, and Zussman (1963, p. 376).

Chemical analysis. A chemical analysis by Booth, Garrett, and Blair, Inc., Philadelphia, Pennsylvania, of crystals from which the structure was determined is given in Table 1. The chemical formula of heulandite based on 72 oxygen atoms in the anhydrous cell is

$$Ca_{3.5}Sr_{0.4}K_{0.9}Al_{9.3}Si_{26.8}O_{72} \cdot 26.1\ H_2O$$

The unit cell contains four formula weights of the ideal formula (Ca, Na_2) $Al_2Si_7O_{18} \cdot 6H_2O$.

TABLE 1. CHEMICAL ANALYSIS OF HEULANDITE

Oxide	Percent
SiO_2	57.38
Al_2O_3	16.91
CaO	7.00
K_2O	1.38
SrO	1.55
Na_2O	0.10
MgO	0.01
H_2O (+)	13.67
H_2O (−)	3.06
Total	101.06

Powder diffraction data. An X-ray powder diffraction photograph was made from the heulandite sample using Ni-filtered Cu radiation. Table 2 shows the diffraction data of heulandite indexed on the basis of its true monoclinic cell.

TABLE 2. X-RAY POWDER DATA FOR HEULANDITE

d_{obs} (Å)	d_{calc}	I (rel.)	hkl	d_{obs} (Å)	d_{calc}	I (rel.)	hkl
8.845	8.909	80	(020)	2.270	2.267	10	($\bar{6}03$)
7.796	7.945	70	(200)	2.196	2.197	10	($\bar{6}23$)
6.631	6.659	60	(001)	2.120	2.120	20	(730)
5.945	5.930	10	(220)	2.078	2.077	20	($\bar{1}72$)
5.277	5.256	50	($\bar{3}11$)	2.010	2.011	20	($\bar{7}52$), ($\bar{7}53$)
5.096	5.077	70	(310)	1.963	1.963	30	($\bar{8}41$), ($\bar{5}72$)
4.646	4.639	60	($\bar{1}31$)	1.850	1.851	10	(082)
4.364	4.369	20	($\bar{4}01$)	1.814	1.814	10	(840)
3.917	3.923	100	(421)	1.770	1.771	30	($\bar{1}02$), (243)
3.723	3.726	20	($\bar{2}41$)	1.722	1.722	10	($\bar{2}101$), (0101)
3.562	3.565	20	($\bar{3}21$)	1.698	1.698	20	($\bar{9}51$), ($\bar{1}021$)
3.420	3.428	70	($\bar{2}22$)	1.662	1.665	10	(004)
3.320	3.329	10	(002)	1.639	1.639	10	($\bar{5}54$), (024)
3.186	3.177	50	($\bar{4}22$)	1.608	1.607	10	(713), ($\bar{2}102$)
3.132	3.129	40	(510)	1.585	1.585	10	($\bar{1}43$)
2.959	2.957	90	(350)	1.561	1.561	10	($\bar{1}54$), ($\bar{8}81$), ($\bar{8}82$)
2.805	2.802	70	(530), ($\bar{6}21$)	1.512	1.512	10	($\bar{1}93$), ($\bar{1}\bar{1}31$)
2.730	2.735	40	($\bar{5}32$)	1.473	1.473	10	($\bar{5}111$), ($\bar{1}063$)
2.667	2.667	10	(042)	1.449	1.449	10	($\bar{7}93$), (0121)
2.529	2.531	20	($\bar{1}52$)	1.431	1.431	10	($\bar{1}\bar{1}51$)
2.430	2.430	30	(261), (441), ($\bar{7}12$)	1.401	1.401	10	(1060), ($\bar{6}103$)
2.350	2.350	10	($\bar{2}23$)	1.360	1.360	10	($\bar{1}\bar{1}05$)

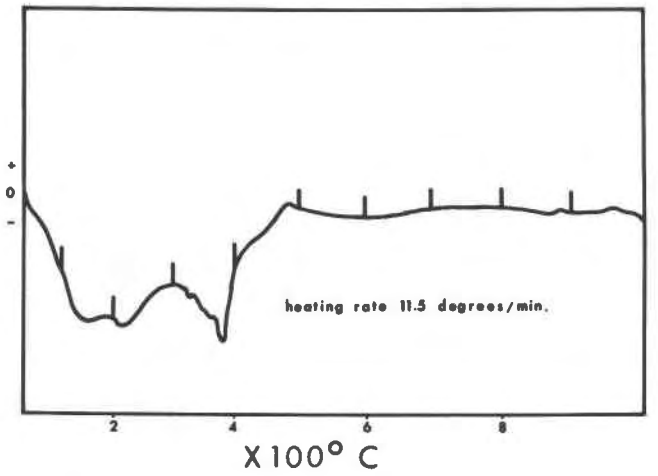

FIG. 1. Differential thermal analysis curve for heulandite.

Differential thermal analysis. The differential thermal analysis curve (Fig. 1) from the heulandite specimen of this study is very similar to other differential thermal curves for heulandite recorded by Mason and Sand (1960) and Mumpton (1960). Endothermic peaks for heulandite occurring at approximately 215° and 372°C, represent the loss of water from the channels. The endothermic peak at 215°C marks the transition to "heulandite B" (Slawson, 1925). Exothermic peaks at 300°C and 480°C mark the formation of wairakite-quartz and anorthite-quartz phases respectively (Koizumi and Roy, 1960).

Unit-cell dimensions and volume. Cell dimensions obtained from precession, rotation, and Weissenberg photographs are monoclinic, $a=17.73$, $b=17.82$, $c=7.43$ Å and $\beta=116°20'$. Heulandite has a pseudo-orthorhombic unit cell which has dimensions of $a=7.43$, $b=17.82$, $c=15.88$ Å with $\beta=91°26'$. Figure 2 shows the relationship between the monoclinic and pseudo-orthorhombic unit cells of heulandite. A unit cell volume of 2103.36 $(Å)^3$ was calculated from the monoclinic cell dimensions of heulandite.

Collection of intensity data. Two methods were employed to obtain intensity data required to determine the crystal structure of heulandite. Photographic data were collected on a Weissenberg camera with the equi-inclination geometry and developed and measured with a modified version of the photoreversal technique proposed by Macintyre and Thompson (1960). Data obtained by this technique were used to determine an

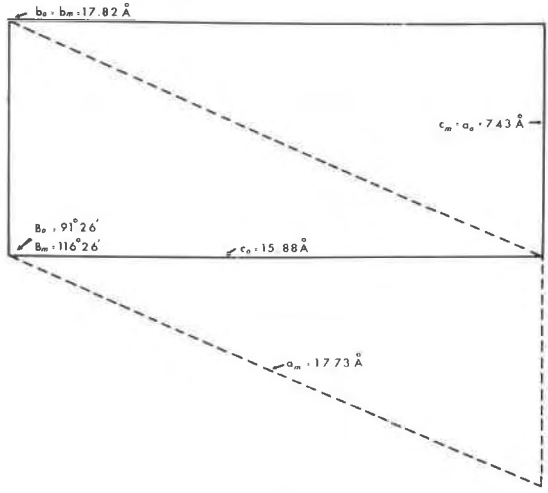

FIG. 2. Relationship between the monoclinic and pseudoorthorhombic unit cells of heulandite.

unrefined structure for heulandite (Merkle and Slaughter, 1967). Data were collected from two book-shaped single crystals having approximate dimensions of 0.46×0.43×0.13 mm. One was mounted on the *b*-axis the other on the *c*-axis. Nine levels of data from the pseudoorthorhombic *b*-axis mounting, and six levels of data from the pseudo-orthorhombic *c*-axis mounting were gathered. Single crystal photographs showed no evidence of twinning or disordering.

To improve accuracy, all data for the structural refinement of heulandite were regathered using a Supper single-crystal x-ray diffractometer. The same book-shaped heulandite crystals, mounted on the pseudo-orthorhombic axes, used in the preliminary work, were used to gather data for the refinement. In all, 1400 independent reflections were measured from 19 levels (*h*0*l* through *h*.18.*l*) on this crystal. The measured reflections comprise approximately 75 percent of the total number of reflections in the CuKα limiting sphere.

Correction of observed intensities. All intensities were scaled and corrected for Lorentz-polarization and absorption effects using IBM 1620 computer programs.[1] Corrected intensities were then transformed from the pseudo-orthorhombic to the monoclinic cell.

[1] IBM 1620 programs by Beurskens, P. T. and R. SHIONO, and in part by D. HALL and S. C. CHU (1963), The Crystallography Laboratory, The University of Pittsburgh, Pittsburgh 13, Pa. See also Kane (1963).

Determination of the Crystal Structure

Determination of the space group. Single crystal Weissenberg and precession photographs of heulandite show monoclinic symmetry with extinctions of the type $h+k=2n+1$ for the general reflections (hkl) indicating the space group $C2/m$, Cm, or $C2$. The zero-moment centricity test (Howells, Phillips, and Rogers, 1950) Figure 3, with ($h0l$) and ($hk0$) reflections suggest the mineral is not centrosymmetric, reducing space group choices to the noncentric groups Cm or $C2$.

The positions of atoms retrieved by the minimum function, as well as a

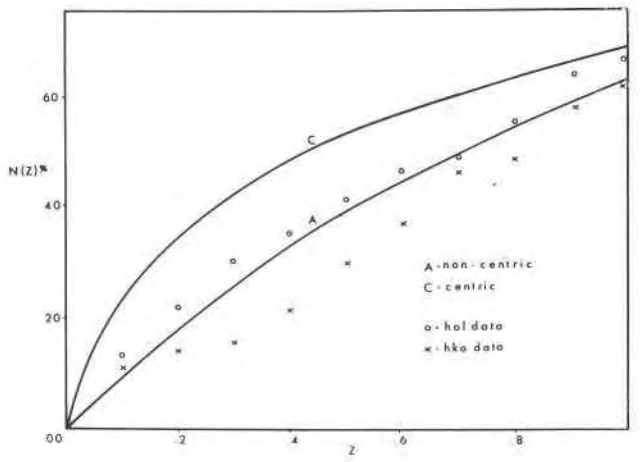

Fig. 3. Heulandite zero-moment centricity test.

high density of peaks in the Patterson function along the line 0, y, 0, implied that heulandite has a mirror symmetry and space group Cm.

Determination of the trial structure. A set of three dimensional Patterson maps was interpreted using techniques based on the intersection function, vector convergence, and the visual estimation of a minimum function (Buerger, 1959, p. 239). A similar two-dimensional technique has been previously used and described in detail by Slaughter (1962, p. 23).

The modified minimum function, as it has been used in the structural analysis of heulandite, retrieved silicon positions from the 0.00, 0.10, 0.20, and 0.40 Patterson levels on the b-axis.

The atomic positions retrieved by application of the modified minimum function combined with positions deduced from knowledge that the 7.43 Å c-axis dimension of heulandite is indicative of a parallel 8-member tetrahedral ring were as follows:

Atom	*x*	*y*	*z*
Si_1	.10	.19	.40
Si_2	.00	.09	.00
Si_3	.08	.19	.78
O_1	.00	.00	.00
O_2	.06	.13	.90
O_3	.10	.19	.60
O_4	.04	.13	.23

The remainder of the framework atoms, calcium ions and water molecules were located by successive Fourier syntheses. Introduction of all framework atoms reduced the discrepancy index, R:

$$R = \frac{\sum ||F_0| - |F_c||}{\sum |F_0|},$$

from an initial value of 0.52 to 0.30. Positioning the Ca ions reduced R to 0.25, and placing waters reduced R to 0.20. The coordinates of the unrefined structure excluding some waters have been given by Merkle and Slaughter (1967).

Refinement of the crystal structure. The structure of heulandite was refined by a combination of differential Fourier synthesis and least-squares techniques. A discrepancy index of 0.20 was calculated for heulandite using unrefined coordinates for the silicate framework and cations, intensity data collected using a Supper single-crystal diffractometer, and programs for the IBM 1620 computer written by Slaughter (1964).

Addition of all water molecules and four cycles of differential synthesis refinement with manual adjustment of temperature and site occupancy factors reduced the discrepancy index to 0.15. Calculated and observed values of the electron densities, temperature factors, and curvatures indicated partial occupancy of aluminum in silicon positions 1, 2, 4, 7, and 9 (Tables 3 and 4). Two more cycles of differential synthesis with partial aluminum added to these positions lowered the discrepancy index to 0.14. Bond distances improved after adding aluminum atoms.

Further refinement was made using an IBM 7040 computer and the Busing, Martin, and Levy (1962) least-squares refinement program. Because least-squares technique would not handle positions partially occupied by aluminum and silicon, all tetrahedra were considered to be occupied by silicon. Three cycles of least-square refinement reduced the discrepancy index, R, from 0.15 to 0.14, and to a weighted R of 0.11.

Table 3 lists the final atomic coordinates, standard deviations, site occupancy, and temperature factors for all independent atoms in the heulandite structure. Table 4 lists the interatomic distances for atoms in

TABLE 3. FINAL ATOMIC PARAMETERS AND STANDARD DEVIATIONS FROM LEAST-SQUARES REFINEMENT

Atom	x	y	z	Occupancy[a]	Temperature Factors	
					Least squares	Differential synthesis
Si, Al (1)	0.1075	0.1693	0.4049	0.75, 0.25	1.32	0.83
Si, Al (2)	.9968	.9096	.0056	.25, .75	1.83	.79
Si (3)	.0773	.1917	.7880	1.0	1.24	.82
Si, Al (4)	.3488	.3020	.9107	.60, .40	1.23	.83
Si (5)	.2852	.2152	.5075	1.0	1.14	.80
Si (6)	.4907	.1907	.2188	1.0	.89	.79
Si, Al (7)	.4652	.1708	.5978	.75, .25	.68	.83
Si (8)	.2204	.2990	.0899	1.0	1.35	.80
Si, Al (9)	.0714	.4104	.0043	.25, .75	.76	.77
σ	.002	.001	.004			
Ox (1)	.9820	.0000	.9746	1.0	3.01	2.80
Ox (2)	.0626	.1202	.8931	1.0	1.80	2.20
Ox (3)	.0966	.1499	.6104	1.0	3.33	1.90
Ox (4)	.0456	.1087	.2566	1.0	1.97	1.80
Ox (5)	.2851	.3318	.0077	1.0	2.21	1.80
Ox (6)	.2069	.1621	.4386	1.0	1.83	1.60
Ox (7)	.1552	.2425	.9541	1.0	4.07	2.25
Ox(8)	.2951	.2685	.6890	1.0	2.34	2.15
Ox (9)	.0717	.2552	.3240	1.0	1.66	1.80
Ox (10)	.2775	.2646	.3196	1.0	2.60	2.00
Ox (11)	.3666	.1613	.5673	1.0	1.62	1.60
Ox (12)	.0175	.3984	.7552	1.0	2.45	1.80
Ox (13)	.0933	.5000	.0873	1.0	3.03	2.80
Ox (14)	.4608	.1575	.3774	1.0	.36	2.00
Ox (15)	.4978	.2551	.6450	1.0	3.51	2.30
Ox (16)	.4085	.3758	.9159	1.0	4.30	1.95
Ox (17)	.0198	.3812	.1167	1.0	3.42	1.80
Ox (18)	.1699	.3746	.1234	1.0	1.31	2.10
Ox (19)	.4100	.2328	.0553	1.0	1.82	1.85
σ	.003	.003	.007			
HOH (1)	.9957	.0000	.4686	1.0	.88	2.80
HOH(2)	.0388	.5000	.4648	1.0	1.13	2.90
HOH (3)	.2005	.4079	.5270	1.0	4.89	4.25
HOH (4)	.2765	.5000	.9634	1.0	5.98	4.35
HOH (5)	.3545	.4267	.4683	1.0	5.25	4.20
HOH (6)	.3665	.0000	.7543	1.0	3.17	4.20
HOH (7)	.1548	.0000	.1553	.30	4.20	4.20
HOH (8)	.1985	.0000	.5998	.32	4.00	4.00
HOH (9)	.2882	.1001	.0552	.30	4.10	4.10
HOH (10)	.3628	.0000	.4000	.18	4.10	4.10
HOH (11)	.2898	.0000	.3030	.15	4.10	4.10
σ	.003	.005	.008			
Ca (1)	.1417	.0000	.8478	.34	2.95	2.77
Ca (2)	.4355	.0000	.1776	.38	3.91	2.77
Ca (3)	.2403	.5000	.2989	.48	2.35	2.33
σ	.002		.005			

[a] Occupancy determined from differential synthesis.

TABLE 4. INTERATOMIC DISTANCES

Atom Pair		Distance in Å
Si, Al (1)	-Ox (3)	1.66
	Ox (4)	1.58
	-Ox (6)	1.67
	-Ox (9)	1.66
Mean		1.64
Si, Al (2)	-Ox (1)	1.65
	-Ox (2)	1.69
	-Ox (4)	1.70
	-Ox (16)	1.62
Mean		1.66
Si (3)	-Ox (2)	1.58
	-Ox (3)	1.68
	-Ox (7)	1.65
	-Ox (15)	1.58
Mean		1.62
Si, Al (4)	-Ox (5)	1.67
	-Ox (8)	1.61
	-Ox (16)	1.68
	-Ox (19)	1.68
Mean		1.66
Si (5)	-Ox-(6)	1.57
	-Ox (8)	1.59
	-Ox (10)	1.60
	-Ox (11)	1.62
Mean		1.60
Si (6)	-Ox (9)	1.61
	-Ox (14)	1.60
	-Ox (17)	1.68
	-Ox (19)	1.59
Mean		1.62
Si, Al (7)	-Ox (11)	1.67
	-Ox (12)	1.67
	-Ox (14)	1.62
	-Ox (15)	1.64
Mean		1.65
Si (8)	-Ox (5)	1.63
	-Ox (7)	1.53
	-Ox (10)	1.67
	-Ox (18)	1.70
Mean		1.63
Si, Al (9)	-Ox (12)	1.68
	-Ox (13)	1.69
	-Ox (17)	1.58
	-Ox (18)	1.69
Mean		1.66

Si, Al (1)	Ox (3)	–Ox (4)	2.48
	Ox (3)	–Ox (6)	2.78
	Ox (3)	–Ox (9)	2.72
	Ox (4)	–Ox (6)	2.73
	Ox (4)	–Ox (9)	2.66
	Ox (6)	–Ox (9)	2.72
Si, Al (2)	Ox (1)	–Ox (2)	2.79
	Ox (1)	–Ox (4)	2.71
	Ox (1)	–Ox (16)	2.51
	Ox (2)	–Ox (4)	2.85
	Ox (2)	–Ox (16)	2.81
	Ox (4)	–Ox (16)	2.63
Si (3)	Ox (2)	–Ox (3)	2.49
	Ox (2)	–Ox (7)	2.64
	Ox (2)	–Ox (15)	2.66
	Ox (3)	–Ox (7)	2.82
	Ox (3)	–Ox (15)	2.67
	Ox (7)	–Ox (15)	2.61
Si, Al (4)	Ox (5)	–Ox (8)	2.70
	Ox (5)	–Ox (16)	2.68
	Ox (5)	–Ox (19)	2.73
	Ox (8)	–Ox (16)	2.74
	Ox (8)	–Ox (19)	2.65
	Ox (16)	–Ox (19)	2.75
Si (5)	Ox (6)	–Ox (8)	2.63
	Ox (6)	–Ox (10)	2.58
	Ox (6)	–Ox (11)	2.56
	Ox (8)	–Ox (10)	2.62
	Ox (8)	–Ox (11)	2.66
	Ox (10)	–Ox (11)	2.59

TABLE 4—(*Continued*)

Atom Pair		Distance in Å	Atom Pair		Distance in Å	
Si (6)	Ox (9) –Ox (14)	2.67	Ca (1)	-Ox (1)	3.36	
	Ox (9) –Ox (17)	2.65		-Ox (2)	2.66	
	Ox (9) –Ox (19)	2.68		-Ox (2)	2.66	
	Ox (14)–Ox (17)	2.67		-HOH (1)	2.79	
	Ox (14)–Ox (19)	2.54		-HOH (7)	2.19	(2.26)[a]
	Ox (17)–Ox (19)	2.71		-HOH (8)	2.46	
				-HOH (9)	2.96	
Si, Al (7)	Ox (11)–Ox (12)	2.63		-HOH (9)	2.96	
	Ox (11)–Ox (14)	2.62				
	Ox (11)–Ox (15)	2.68	Ca (2)	-Ox (13)	3.15	
	Ox (12)–Ox (14)	2.72		-Ox (17)	2.74	
	Ox (12)–Ox (15)	2.78		-Ox (17)	2.74	
	Ox (14)–Ox (15)	2.71		-HOH (2)	2.11	(2.28)[a]
				-HOH (6)	2.82	
Si (8)	Ox (5) –Ox (7)	2.68		-HOH (9)	2.95	
	Ox (5) –Ox (10)	2.66		-HOH 10)	2.51	
	Ox (5) –Ox (18)	2.66		-HOH (9)	2.95	
	Ox (7) –Ox (10)	2.65				
	Ox (7) –Ox (18)	2.63	Ca (3)	-Ox (13)	2.37	
	Ox (10)–Ox (18)	2.67		-Ox (18)	2.61	
				-Ox (18)	2.61	
Si, Al (9)	Ox (12)–Ox (13)	2.86		-HOH (3)	2.67	
	Ox (12)–Ox (17)	2.69		-HOH (4)	2.84	
	Ox (12)–Ox (18)	2.89		-HOH (5)	2.26	(2.42)[a]
	Ox (13)–Ox (17)	2.55		-HOH (3)	2.67	
	Ox (13)-Ox (18)	2.57		-HOH (5)	2.26	(2.42)[a]
	Ox (17)–Ox (18)	2.64				

[a] Bond distance determined from differential synthesis.

the structure. Observed and calculated structure factors are available from the authors on request.

DISCUSSION OF THE STRUCTURE

The tetrahedral framework. Heulandite, a complex hydrated calcium aluminum silicate, is characterized by an open framework of silicon and aluminum atoms surrounded tetrahedrally by oxygen atoms; each tetrahedron is tied to another by a shared oxygen atom. Channels in this framework are filled by weakly held water molecules and cations, both of which may be removed or exchanged by other molecules without destroying or altering the silicate framework. Cations in the heulandite structure are bonded to oxygens of aluminum-substituted tetrahedra and surrounded by coordination waters.

Taylor (1934) originally described the heulandite structure as probably being composed of a layering of silicate tetrahedra infinite in two directions, and finite in thickness. Ventriglia (1955) proposed a different structural arrangement for this zeolite. The heulandite structure determined in this study is completely different from that of Ventriglia and is consistent with Taylor's original structural concept.

The crystal structure of heulandite is characterized by large, intersecting, relatively open channels of 10- and 8-member tetrahedral rings. The axes of these channels lie in the *ac*-crystallographic plane parallel to the monoclinic *c*-axis of heulandite and both parallel and at a 50° angle to its monoclinic *a*-axis. The channels are bisected by the mirror plane at heights of 0.00 and 0.50 on the *b*-crystallographic axis, and are linked by a complex layer arrangement of 6-, 5- and 4-member tetrahedral ring groups at heights of 0.25 and 0.75 on the *b*-crystallographic axis. The excellent (010) cleavage in heulandite is caused by the alternate layering of open channels and complex linkages. Cations present in the heulandite structure are distributed over three positions in the channels, associated with framework oxygen atoms, and surrounded by water molecules. The absence of large openings in the tetrahedral layers restricts ionic migration and exchange to the *ac*-crystallographic plane.

As stated by Zoltai and Buerger (1960) the relative energy of 5- and 6-member tetrahedral rings is low, thus favoring their stability over other types of tetrahedral ring arrangements. The presence of numerous 5- and 6-member tetrahedral rings in the structure accounts for the relative abundance and stability of heulandite in nature.

Figure 4, a schematic drawing of part of the heulandite structure in the monoclinic *b*–*c* plane, the pseudo-orthorhombic *c*-axis, shows silicate tetrahedra forming a layer-like assemblage of 8-, 6- and 4-member ring groups. The layers are complexly connected by additional silicate tetrahedra, and offset in the monoclinic *c*-direction by an amount equal to approximately one-half the *c*-dimension. The offset nature of superjacent layers effectively closes the channels and restricts ionic movement. The (010) cleavage plane of heulandite bisects the 8-member ring channels at heights of $b = 0.00$ and 0.50.

Figure 5, a photograph of the heulandite model in the pseudo-orthorhombic *b*–*c* plane, shows open 10- and 8-member ring channels held together by a complex layering of 6-, 5-, and 4-member ring groups. The 10-member ring channel parallel to the monoclinic *c*-axis is the only unrestricted channel in heulandite.

Substitution of aluminum for silicon. During differential synthesis refinement employing manual adjustment of temperature factors, the tempera-

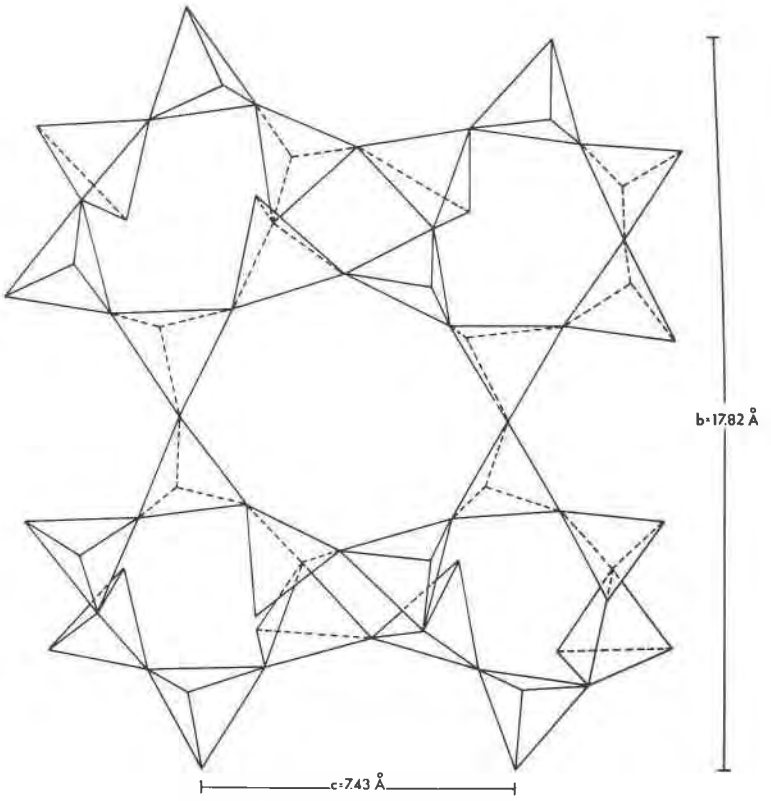

FIG. 4. Schematic view of part of the framework viewed perpendicular to the pseudo-orthorhombic *c*-axis of heulandite showing 8-member ring channels, the plane formed by 8-, 6-, and 4-member ring groups, and the (010) cleavage.

ture factors for five of the nine independent silicon atoms became noticeably higher than the others. The observed electron density values for these silicon positions were less than the values at the other silicon sites. Oxygen atoms associated with these five silicon positions had greater than normal Si-O bond distances (Table 4). Therefore, these sites were considered to be partially occupied by aluminum.

Over half of the aluminum in heulandite is distributed equally over the two silicate tetrahedra (2 and 9, Table 3) which hold the individual layers of heulandite together. The occupancy by aluminum is approximately 75 percent in each of these positions. The remainder of the aluminum is distributed over three silicate tetrahedra (4, 1, and 7, Table 3) occurring within the tetrahedral layers. The occupancy by aluminum in these tetrahedra is 40, 25 and 25 percent respectively. The presence of alumi-

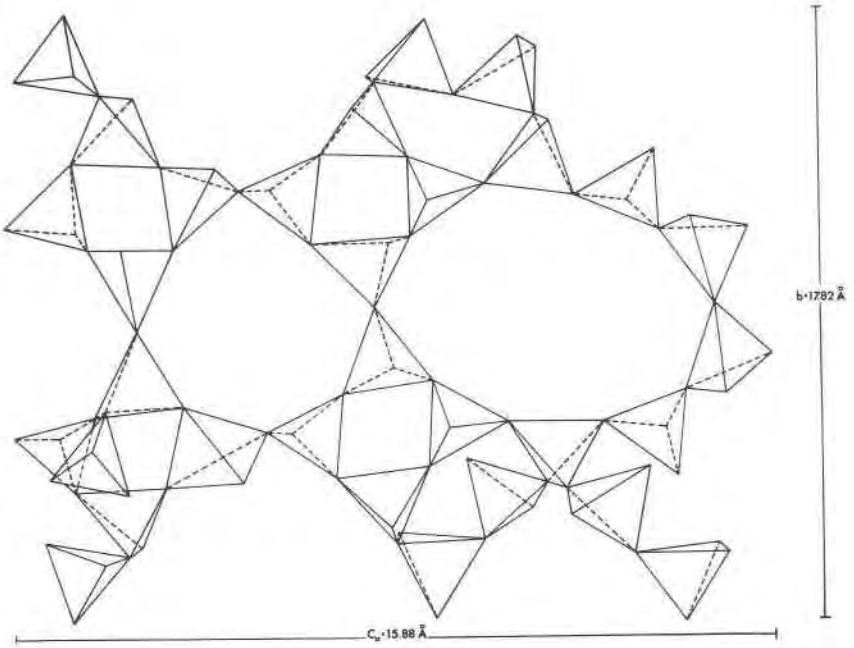

FIG. 5. Schematic drawing of the framework approximately parallel to the pseudo-orthorhombic *bc* plane of heulandite showing the (010) cleavage, tetrahedral layers, and open channels formed by 10- and 8-member ring groups.

num in tetrahedra (2 and 9) which holds the heulandite layers together seems to directly violate the Al-O-Al avoidance rule since each tetrahedron containing aluminum is connected to an equivalent one across the mirror. All calcium ions are associated with oxygens in aluminum-substituted tetrahedra. The close association of calcium with oxygens in aluminum-substituted tetrahedra is consistent with Pauling's electrostatic valence rule (1960).

In heulandite, most aluminum substitution takes place in tetrahedra 2 and 9 which serve to hold the tetrahedral layers together. Substitution in these tetrahedra is allowed because of energy conditions caused by the structural arrangement of heulandite. Aluminum substitution in tetrahedra 2 and 9 causes the highly electronegative oxygens of these tetrahedra to have an excess of negative charges, compensated for by calcium ions, being as close as possible to these oxygens to minimize the Coulomb energy.

If the major substitution occurred in the tetrahedral layers of heulandite, rather than between layers, stronger Coulombic repulsive forces would result because of the close proximity of second neighbor oxygens in

the 4-member rings. Furthermore, the distance between these substituted tetrahedra and the cations would be great, thereby reducing the electrostatic attraction energy. In heulandite substitution in the tetrahedral layers would most certainly result in a higher potential energy than that of the observed configuration.

The tetrahedral layers of heulandite contain contracted and expanded 4-member ring groups. Minor substitution of aluminum occurs in alternate tetrahedra 1, 4, and 7 of the expanded 4-member ring groups. The resultant Coulombic energy should be lower than the Coulombic energy which would be caused by substitution in tetrahedra from the contracted 4-member ring groups. In heulandite all aluminum-substituted tetrahedra occur in framework positions which bracket the calcium ions, thus minimizing the Coulomb energy.

Bond distances (Table 4) calculated for the aluminum-substituted tetrahedra give Si, Al-O distances of approximately 1.66 Å whereas normal Si-O distances are about 1.62 Å (Smith and Bailey (1963).

Bond distances based on coordinates refined by the least-squares technique (Table 4) again confirm the presence of partial aluminum in five silicon positions (1, 2, 4, 7, and 9).

Cation-water-framework-relationships. In heulandite, calcium is distributed over three special positions on the mirror. These calcium atoms occur in the open channels near the intersection of 10- and 8-member rings and two 8-member rings. Relationships between the calcium framework, and water molecules are shown in Figure 7. Each calcium is coordinated to three framework oxygen atoms from aluminum-substituted tetrahedra and five water molecules which occupy general and special positions in the channels. Because of unequal distribution of the calcium, not all water sites have full occupancy.

Calcium atoms 1 and 2 are similar in their relationships to the framework oxygens and water molecules. The calcium atom is in eightfold coordination with three framework oxygens and five water molecules and located at the intersection of the 10- and 8-member tetrahedral ring channels. Because calcium atoms 1 and 2 are closely associated with aluminum-substituted silicate tetrahedra, calcium atoms occur near the sides of the open channels rather than in the middle (Figures 8 and 10). Both calcium 1 and 2 are coordinated to three water molecules and one framework oxygen lying on the mirror, and two framework oxygens and two water molecules, one of each lies above and the other below the mirror plane (Figure 7). The coordinating waters form square antiprisms.

Calcium 3 occurs at the intersection of two 8-member ring channels. To bring it closer to the framework oxygens, calcium 3 lies slightly toward

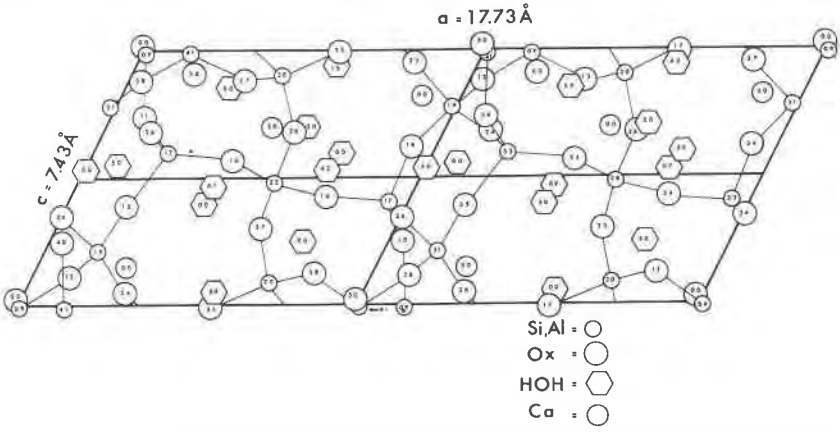

FIG. 6. Projection of all atoms in the half cell of heulandite on the (010) plane. Each number on an atom indicates its y-coordinate.

the sides rather than in the middle of the channels. Calcium 3 is also in eightfold coordination with three framework oxygens and 5 water molecules. However, only one water molecule and one framework oxygen lie on the mirror plane; the remaining two oxygens and four water molecules lie above and below the plane (Figure 7). The four water molecules coordinated to calcium 3 are closely associated with aluminum-substituted tetrahedra (Figure 6).

In each calcium-water-framework relationship three of the five coordinated water molecules lie at a greater distance from the calcium than the other two, implying that two of the water molecules are more tightly held by the calcium than the other three.

Figure 8, a map of the mirror plane, in heulandite shows all channel

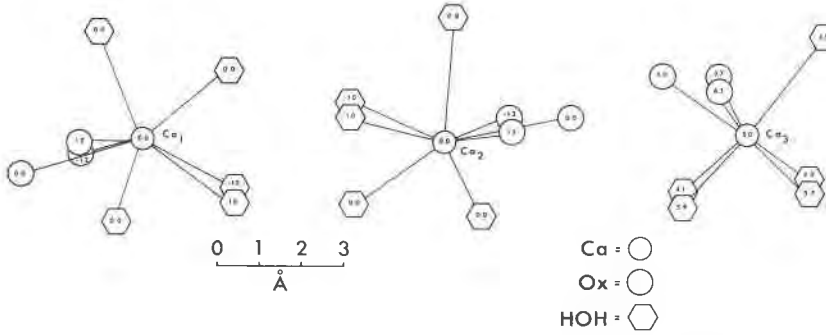

FIG. 7. Environments surrounding each of the calcium positions in heulandite. The number on each atom indicates the y-coordinate of the atom.

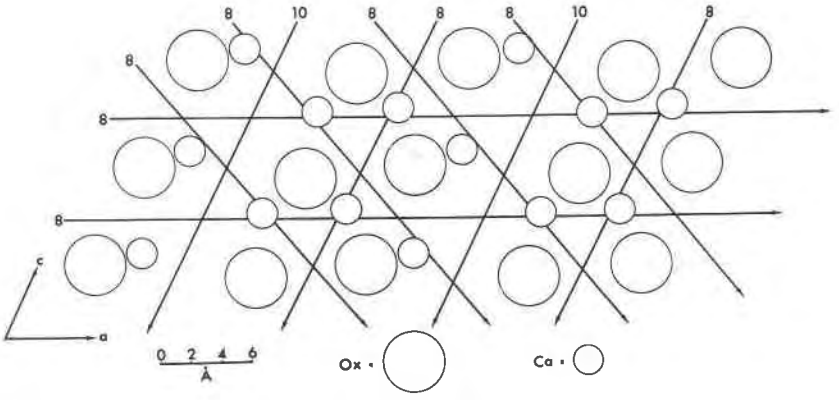

FIG. 8. Map view of atoms on the plane (x, 0, z) in heulandite showing channel directions, number of tetrahedra in each forming the channels, and positions of calcium in the channels.

directions and indicates the number of tetrahedra that comprise the rings forming these channels. Calcium atoms are shown in their proper positions near the intersection of two channels. Figure 8 also illustrates that the 10-member ring channel parallel to the c-axis is the only relatively open channel in heulandite; all other channels are blocked by the presence of tightly held calcium.

In general, it may be said all channels in heulandite have elliptical cross sections. Channel dimensions in heulandite are calculated using the coordinates of oxygen atoms forming each channel, an oxygen radius of 1.40 Å, and the unit-cell dimension of heulandite. Open channels in the monoclinic c-direction of heulandite are comprised of 10- and 8-member rings. Approximate dimensions for the 10-member ring channels are 7.05×4.25 Å; dimensions for the 8-member ring channels are 4.60×3.95 Å. The 8-member ring channels lying parallel to the monoclinic a-axis have an effective diameter of approximately 5.40×3.90 Å. Channels lying at an angle of approximately 50° to the monoclinic a-axis of heulandite are formed by 8-member rings and have dimensions of 5.20×3.90 Å. Stronger bonding due to the association of calcium with charge deficient aluminum tetrahedra probably restricts the ability of heulandite to undergo ionic exchange.

Relationship of differential thermal analysis to the structure. The determination of the crystal structure of heulandite leads directly to a more complete interpretation of its DTA pattern. The DTA pattern of heulandite (Figure 1) shows two prominent endothermic peaks occurring in the temperature ranges 150°–225°C and 350°–400°C each associated with

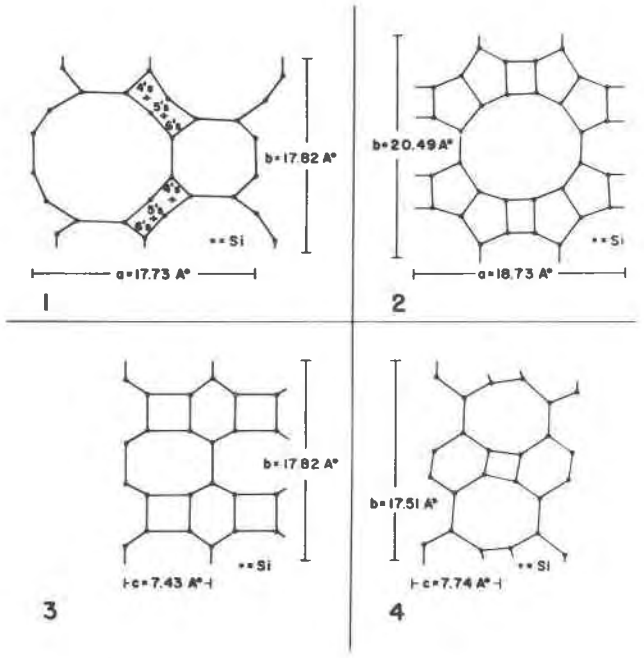

FIG. 9. Composite figure showing the structural similarities between the *ab*-crystallographic plane of heulandite (1) the *ab*-plane of mordenite (2), the *bc*-crystallographic plane of heulandite (3), and the *bc*-plane of brewsterite (4).

water loss. Two of the five water molecules are coordinated more closely to each calcium atom than are the other three, approximately half of the water in heulandite is more tightly bonded than the remainder. The first endothermic peak in heulandite indicates the loss of weakly held water molecules (1, 4, 6, 9, and 11) reducing the coordination on each calcium from 8 to 5. The second endothermic peak marks the loss of the remainder of the water in heulandite.

Relationship to other zeolites. The heulandite group of zeolites as described by Deer, Howie, and Zussman (1963) is comprised of heulandite, stilbite, epistilbite, dachiardite, ferrierite, and brewsterite. Smith (1963) in his classification of zeolites describes the mordenite group including mordenite and dachiardite. Because of similar 7.50 Å spacings, Smith believes the zeolites heulandite, brewsterite, ferrierite, and laumontite could be related to the mordenite group by different ways of cross linking the chains of 5-member rings present in mordenite.

The solution of the crystal structure of heulandite shows it is composed of a layered tetrahedral arrangement and Smith is correct in an assump-

tion that the crystal structure of heulandite is not based on the column arrangement of 5-member rings in mordenite. Indeed, heulandite contains numerous 5-member rings; however, they are combined with 6-, and 4-member rings to form well defined layers infinite in two dimensions.

A study of the unit-cell dimensions of these zeolites shows each has some similar dimensions leading one to believe that structural similarities very likely exist between these minerals. The crystal structure of mordenite (Meier, 1961), dachiardite (Gottardi and Meier, 1963), brewsterite (Perrotta and Smith, 1964), and epistilbite (Slaughter and Kane, 1967) have already been determined. The solution of the crystal structure of heulandite shows this mineral is related to mordenite, dachiardite, and brewsterite; its relationship to epistilbite is minor. The *bc*-crystallographic planes of heulandite ($b=17.82$ Å, $c=7.43$ Å) and brewsterite ($b=17.51$ Å, $c=7.74$ Å) are similar in spacing and tetrahedral arrangements. Both zeolites have similar arrangements of 8-, 6-, and 4-member tetrahedral ring groups. The mirror plane in heulandite is observed at height 0.000 and 0.50 on *b*, whereas the mirror plane in brewsterite is present at height 0.25 and 0.75 on *b*. The similarities between these structures may easily be seen by comparing parts 3 and 4 of Figure 9. The *ab*-crystallographic planes of heulandite and mordenite ($a=18.13$ Å, $b=20.49$ Å) are similar, in that both contain 12- and 8-member rings. In heulandite these rings are linked by layers of complex 6-, 5- and 4-member ring groups; whereas in mordenite they are surrounded and linked by columns of 5- and 4-member ring groups. Similarities between heulandite and mordenite may be seen by comparing parts 1 and 2 of Figure 9.

Acknowledgment

The authors would like to thank the National Science Foundation for financial support for this study (Grant number NSF GP 470).

References

Buerger, Martin J. (1959) *Vector Space and its Application in Crystal-structure Investigation.* John Wiley and Sons, New York, 347 p.

Busing, W. R., K. O. Martin and H. A. Levy (1962), Oak Ridge least-squares program. *Clearinghouse, U. S. Fed. Sci. Tech. Info.* **ORNL-TM-305.**

Coombs, D. S., A. D. Ellis, W. S. Fyfe, and A. M. Taylor (1959) The zeolite facies, with comments on the interpretation of hydrothermal synthesis. *Geochim. Cosmochim Acta* **17,** 53–107.

Deer, W. A., R. A. Howie, and J. Zussman (1963) *Rock-forming Minerals.* **4,** John Wiley and Sons, New York, 435 p.

Gottardi, G., and W. M. Meier (1963) The crystal structure of dachiardite. *Z. Kristallogr.* **119,** 53–64.

Howells, E. R., D. C. Phillips and D. Rogers (1950) The probability distribution of x-ray intensities. II. Experimental investigation and the x-ray detection of centers of symmetry. *Acta Crystallogr.* **3,** 210–214.

KANE, W. T. (1966) *The Crystal Structure of Epistilbite.* Ph.D. Thesis, University of Missouri, Columbia, Mo.

KOIZUMI, M. AND R. ROY (1960) Zeolite studies. I. Synthesis and stability of the calcium zeolites. *J. Geol.* **68,** 41–53.

MACINTYRE, W. M. AND G. THOMSON (1960) Measurement of x-ray intensities from reversed films. *Z. Kristallogr.* **113,** 466–474.

MASON, B., AND L. B. SAND (1960) Clinoptilolite from Patagonia; the relationship between clinoptilolite and heulandite. *Amer. Mineral.* **45,** 341–350.

MERKLE, A. B. AND M. SLAUGHTER (1967) The crystal structure of heulandite *Amer. Mineral.* **52,** 273–276.

MUMPTON F. A., (1960) Clinoptilolite redefined. *Amer. Mineral.* **45,** 351–369.

PAULING. L. (1960) *The Nature of the Chemical Bond.* Cornell University Press, Ithaca, New York, 644 p.

PERROTTA, A. J., AND J. V. SMITH (1964) The crystal structure of brewsterite (Sr, B, Ca) $(Al_2Si_6O_{16})$ $5H_2O$. *Acta Crystallogr.* **17,** 857–862.

SLAUGHTER, M., (1962) *The Crystal Structure of Aluminum Tetroxycarbide.* Ph.D. Thesis, University of Pittsburgh.

——— AND W. T. KANE (1968) The crystal structure of a disordered epistilbite. *Z. Kristallogr.* (in press).

SLAWSON, C. B. (1925) The thermo-optical properties of heulandite. *Amer. Mineral.*, **10,** 305–331.

SMITH, J. V. (1963) Structural classification of zeolites. *Mineral. Soc. Amer. Spec. Pap.* **1,** 281–290.

———, AND S. W. BAILEY (1963) Second review of Al-O and Si-O tetrahedral distances. *Acta Crystallogr.* **10,** 801–811.

TAYLOR, W. H. (1934) The nature and properties of aluminosilicate framework structures. *Proc. Roy. Soc. London, Ser. A.*, **145,** 80–103.

VENTRIGLIA, U. (1955) La struttura della heulandite. *Periodico Mineral., Roma,* **24,** 49–83.

ZOLTAI, T., AND M. J. BUERGER (1960) The relative energies of rings of tetrahedra. *Z. Kristallogr.*, **114,** 1–8.

Manuscript received, May 5, 1967; accepted for publication, February 12, 1968.